Article

Discovery Medicine 2026; 38(211): 2496–2513
https://doi.org/10.24976/Discov.Med.202638211.197

Integration of Bioinformatics and Machine Learning Identifies ENO2 and MPP1 as Shared Molecular Nodes Linking Alzheimer's Disease and Type 2 Diabetes Mellitus

Tingting Li[1,2], Huaizhao Wang[1], Tong Lu[3], Libin Zhan[1,4,5,*]

[1]Key Laboratory of Ministry of Education for TCM Viscera-State Theory and Applications, Liaoning University of Traditional Chinese Medicine, 110847 Shenyang, Liaoning, China
[2]Department of Neurological Rehabilitation I, Affiliated Hospital of Liaoning University of Traditional Chinese Medicine, 110032 Shenyang, Liaoning, China
[3]Emergency Center, Affiliated Hospital of Liaoning University of Traditional Chinese Medicine, 110032 Shenyang, Liaoning, China
[4]College of Basic Medical Sciences, Liaoning University of Traditional Chinese Medicine, 110847 Shenyang, Liaoning, China
[5]Key Laboratory of Liaoning Province for TCM Spleen-Viscera-State Modern Research, 110847 Shenyang, Liaoning, China
*Correspondence: zlblibin2021@163.com (Libin Zhan)
Submitted: 8 June 2026 Revised: 6 July 2026 Accepted: 20 July 2026 Published: 24 August 2026

Background: Alzheimer's disease (AD) is frequently accompanied by type 2 diabetes mellitus (T2DM), and the two disorders share some common pathological mechanisms. However, the core genes responsible for this comorbidity and the therapeutic targets remain to be identified.

Methods: Gene expression data were obtained from the Gene Expression Omnibus (GEO) database for AD (GSE5281) and T2DM (GSE76894), and differentially expressed genes (DEGs) were identified. Weighted gene co-expression network analysis (WGCNA) was performed to identify AD-associated modules. Four machine learning algorithms—Least Absolute Shrinkage and Selection Operator (LASSO) regression, Random Forest (RF), Support Vector Machine Recursive Feature Elimination (SVM-RFE), and Boruta—were used to screen core genes. Gene set enrichment analysis (GSEA), immune infiltration analysis using the CIBERSORT method, and drug prediction using the Comparative Toxicogenomics Database (CTD) were then conducted. In order to evaluate the binding mode and affinity of the predicted drugs with core targets, molecular docking was performed.

Results: The number of DEGs identified in the AD dataset was 4970, and the number of DEGs identified in the T2DM dataset was 392. Cross-analysis of DEGs and WGCNA identified 15 overlapping disease-related genes. Two core genes, enolase 2 (*ENO2*) and membrane palmitoylated protein 1 (*MPP1*), were identified using four machine learning algorithms. Both genes were co-enriched in GSEA for leukocyte transendothelial migration, long-term potentiation/depression, citric acid cycle, oxidative phosphorylation, and glycolysis/gluconeogenesis. Immune infiltration analysis revealed that they participated in the disease process by regulating the immune microenvironment. Valproic acid (VPA) was selected as a candidate drug based on the results of the CTD drug prediction. The molecular docking results revealed that the binding free energies of VPA with *ENO2* and *MPP1* were –4.747 and –5.346, respectively, suggesting that VPA had a higher binding affinity for *MPP1*.

Conclusion: *ENO2* and *MPP1* are shared molecular markers between AD and T2DM, and may be involved in the pathobiology of both diseases by regulating energy metabolism, synaptic function, and immune inflammation. VPA may exert potential therapeutic effects by targeting these two shared nodes, providing preliminary molecular evidence for the mechanisms underlying AD-T2DM comorbidity. Further validation in AD-T2DM comorbid cohorts is warranted.

Keywords: Alzheimer's disease; type 2 diabetes mellitus; machine learning; ENO2; MPP1; molecular docking; valproic acid

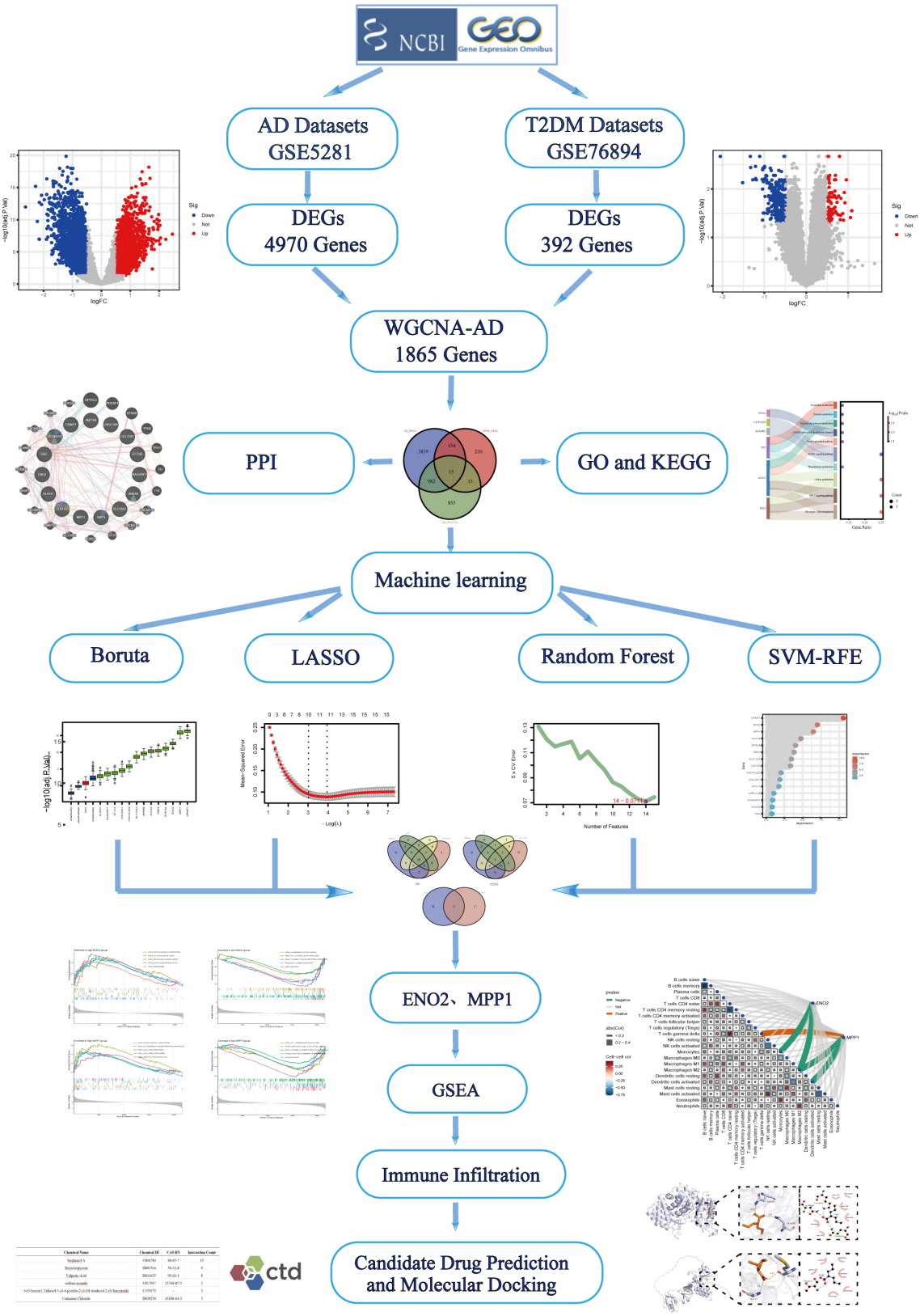

Graphical Abstract

Introduction

The older population is at high risk for two common chronic diseases, Alzheimer's disease (AD) and type 2 diabetes mellitus (T2DM). AD is the most common neurodegenerative disease and is mainly characterized by progressive cognitive impairment and dementia, which are accompanied by a characteristic pathological mechanism of senile plaques (composed of beta-amyloid [Aβ] protein) and neurofibrillary tangles (composed of hyperphosphorylated tau protein) [1]. The prevalence of AD is increasing with the age of the global population. In 2020, more than 58 million people worldwide were affected by AD; by 2050, this is expected to rise to 152 million [2]. T2DM is a chronic metabolic disorder associated with insulin resistance and progressive loss of pancreatic β-cell function, and its prevalence is steadily rising globally. The 11th International Diabetes Federation (IDF) Diabetes Atlas reported that there were 589 million people with diabetes in 2024, which is expected to increase to 853 million by 2050, among people aged 20–79 years [3].

Patients with AD frequently have metabolic disturbances, with the most common being T2DM. In a case-control study, T2DM was found in 35% of the patients with AD and impaired fasting glucose in 46% [4]. According to Lanctôt et al. [5], diabetes is one of the potential metabolic comorbidities in AD patients, ranging from 6.0% to 24.3%. Furthermore, T2DM has been shown to be directly associated with accelerating progressive cognitive decline, and studies have confirmed that T2DM also increases the risk of the onset of AD [6]. A meta-analysis showed that patients with T2DM had a 59% increased risk of all-cause dementia [7]. Conversely, AD can increase the risk of T2DM and contribute to the mortality burden related to comorbidity. In the United States, between 1999 and 2019, the age-adjusted mortality rate for T2DM with comorbid AD among people aged ≥65 years increased from 4.12 to 11.65 per 100,000 population, representing more than a twofold increase [8], which indicates a synergistic health risk when these two conditions co-occur.

Several studies have identified neurobiological crosstalk mechanisms between AD and T2DM. According to Madhusudhanan et al. [9], hyperglycemia, insulin resistance, and oxidative stress are shared mechanisms that contribute to AD progression in patients with T2DM. Diabetes-related symptoms may also be present in patients with AD, and the shared mechanisms include impaired insulin signaling, tau hyperphosphorylation, neuroinflammation, and autophagic dysfunction. Diniz Pereira et al. [10] conducted a systematic review of proteomic studies of AD and T2DM, which revealed 17 proteins differentially expressed between the two diseases, such as apolipoprotein E, α2-macroglobulin, and pancreatic polypeptide, and associated with pathways including cholesterol metabolism, the complement cascade, and fat digestion and absorption. Karki et al. [11] identified the pathway-level crosstalk mechanisms between AD and T2DM using a knowledge-driven network modeling approach, including the insulin signaling, PI3K/AKT, mTOR, and MAPK pathways. Kakkar et al. [12] also listed the major common pathways, comprising impaired insulin signaling, chronic inflammation, oxidative stress, mitochondrial dysfunction, accumulation of Aβ, hyperphosphorylation of tau, and increased levels of advanced glycation end products (AGEs). Despite these advances, the molecular networks and the key genes underlying the co-occurrence of the two are still unclear and should be further investigated.

From a clinical treatment perspective, the most commonly used drugs in the treatment of AD are cholinesterase inhibitors (such as donepezil and rivastigmine) and N-methyl-D-aspartate (NMDA) receptor antagonists (such as memantine). These medications can relieve symptoms but do not prevent disease progression [13]. Some antidiabetic drugs, including metformin [14], sodium-glucose cotransporter 2 inhibitors [15], and glucagon-like peptide-1 receptor agonists [16], have been found to hold promise in the prevention and treatment of AD; nevertheless, further clinical validation is needed to confirm their effectiveness and safety [17]. More importantly, the age-adjusted mortality rate for AD-T2DM comorbidity has increased nearly threefold over the past 20 years [8], and no single therapeutic approach targets both diseases at the same time. Patients with AD-T2DM comorbidities may require treatment by multiple specialists, including neurologists and endocrinologists, and experience the risk of polypharmacy, drug–drug interactions, and poor medication adherence. Therefore, the identification of the molecular targets common to both diseases and the development of the intervention strategy based on a "one drug with multiple effects" approach are of great clinical transformation value.

In this study, a multi-layer integrative bioinformatics approach was used to systematically identify important molecular targets for AD-T2DM comorbidity. Weighted gene co-expression network analysis (WGCNA) was first applied to identify disease-associated gene modules. Second, four complementary machine learning algorithms, Least Absolute Shrinkage and Selection Operator (LASSO) regression, Random Forest (RF), Support Vector Machine Recursive Feature Elimination (SVM-RFE), and Boruta, were combined with differential expression analysis. This combination enabled the identification of core genes using cross-validation. In parallel, immune infiltration analysis was carried out using CIBERSORT. Drug prediction targeting the core genes was performed using the Comparative Toxicogenomics Database (CTD). The binding modes of the candidate drugs with the targets were then validated using molecular docking.

In summary, the present study aims to integrate transcriptomic data from AD and T2DM to identify shared

molecular nodes, evaluate their diagnostic potential, and explore candidate therapeutic compounds using a multi-layer bioinformatics approach combined with machine learning cross-validation.

Methods

Data Sources

To obtain the disease-related gene expression profiles, the search was conducted in the Gene Expression Omnibus (GEO) database with the keywords "Alzheimer's disease" and "type 2 diabetes mellitus". In this study, GSE5281 (87 AD brain samples, 74 control brain samples) and GSE76894 (19 T2DM pancreatic islet samples, 84 control islet samples) were selected.

Differential Expression Analysis

The "limma" package in R was used for the normalization and annotation of the gene expression data. Differentially expressed genes (DEGs) between the AD and control groups as well as between the T2DM and control groups were identified with $|\log2\ FC| \geq 0.5$ and an adjusted p-value < 0.05 [18]. Visualization of the DEGs was performed using heat maps and volcano plots created using R packages such as "ggplot2", "agglomerate", "dplyr", and "pheatmap".

Construction and Analysis of Weighted Gene Co-expression Network

To explore the key genes related to the AD phenotype, we used the "WGCNA" R package to construct the AD and T2DM DEGs-clinical traits subnetwork. Before the analysis, hierarchical clustering was performed using the "hclust" function in R to remove outliers. Subsequently, a scale-free topology was employed to choose the optimal soft-thresholding power β (range 1–20) using the "pickSoftThreshold" function in WGCNA. Topological overlap matrix analysis was used to identify modules, and the module that had the highest correlation was selected as the AD-related module. The online Venn diagram tool (http://bioinformatics.psb.ugent.be/webtools/Venn/) was used to perform intersections between the genes of the AD-related modules.

Functional Enrichment Analysis

To investigate the potential biological roles of the module genes, Gene Ontology (GO) and Kyoto Encyclopedia of Genes and Genomes (KEGG) enrichment analyses were conducted on the module genes using the R package "clusterProfiler". Gene symbols were converted to Entrez Gene IDs based on org.Hs.eg.db, and unmatched genes were excluded. GO enrichment covered Biological Process (BP), Cellular Component (CC), and Molecular Function (MF) with ont = "all" and readable = TRUE. Benjamini–Hochberg (BH) FDR correction was applied, and terms with raw $p < 0.05$ and adjusted $p < 0.05$ were considered significant. GRCh38 human genome-wide protein-coding genes served as the background gene set. KEGG enrichment was used to screen enriched signaling and metabolic pathways, and the top 10 significant enrichment terms were displayed in Sankey bubble plots.

Construction of Gene Functional Interaction Network

The identified core genes were submitted into the GeneMANIA analysis platform (http://genemania.org/) to construct a gene functional interaction network. The species was set as *Homo sapiens*. The network was constructed using four types of functional association evidence: co-expression, physical association, pathway association, and shared protein domains. Additional genes with functional similarity to the input genes were automatically predicted/selected and added to the network to improve the gene interaction results. The co-regulatory relationships between genes were elucidated using the topology of the network, hub genes, and functional module mining. The network consists of nodes representing individual genes, with their size positively correlated with the gene connectivity. The colored lines indicate different types of functional associations: red indicates physical interaction, purple indicates co-expression, light blue indicates pathway association, and light yellow indicates shared protein domains.

Machine Learning Analysis and Validation

Candidate genes were jointly screened using four machine learning algorithms, including LASSO, RF, SVM-RFE, and Boruta, to identify core genes with the highest diagnostic relevance. LASSO regression was performed using an L1-regularized binomial logistic model. A sequence of 100 regularization penalty coefficients (λ) was generated, and 10-fold cross-validation was conducted with deviance as the evaluation metric to determine lambda.min, which yielded the minimum cross-validated deviance. Genes with non-zero coefficients at lambda.min were retained. Random forest was constructed with 500 decision trees using the default mtry parameter. SVM-RFE with a linear kernel was combined with 5-fold internal cross-validation for recursive feature elimination, with halve.above set to 100. The Boruta algorithm was run with a maximum of 500 iterations, and tentative features were reclassified using the TentativeRoughFix function. The intersection of gene sets derived from the four algorithms was obtained using the online Venn diagram tool, yielding the shared core differential genes associated with both Alzheimer's disease and type 2 diabetes. Diagnostic performance was assessed by plotting receiver operating characteristic (ROC) curves and calculating the area under the curve (AUC) using the pROC package. A nomogram was constructed using the rms and regplot packages.

Gene Set Enrichment Analysis (GSEA) of Biomarkers

The core module genes for GSE5281 and GSE76894 were analyzed by GSEA using the R package "clusterProfiler" with a threshold of $p < 0.05$. Significant pathways in the high-expression and low-expression groups were selected for the top five, and enrichment curves were plotted to show the pathway differences between the high-expression and low-expression groups with respect to the expression of the core genes.

Immune Cell Infiltration (ICI) Analysis

To evaluate the ICI abundance, the CIBERSORT deconvolution algorithm was used to analyze ICI based on immune-related gene expression data, estimating the proportions of 22 immune cell types in AD and T2DM samples. Spearman correlation was used to determine the correlations among immune cells and key genes, with $p < 0.05$ deemed statistically significant. The "linkET" package was used to plot the correlation network.

Prediction of Candidate Drugs Targeting Core Genes

Based on the biomarkers associated with AD and T2DM, the CTD was used to screen potential therapeutic compounds. The "Interaction Count" criterion was used for target selection to increase the biological relevance of the identified targets. A stepwise threshold strategy was used for compound screening, while considering the number of candidate compounds and the feasibility of the study [19].

Molecular Docking

The protein structure of *ENO2* was obtained from the Protein Data Bank (PDB) with ID 1TE6 [20]. The protein structure of *MPP1* was retrieved from the AlphaFold Protein Structure Database (Uniprot ID: Q00013, model version: AlphaFold DB v4). All protein structures were processed using ADFRsuite-1.0 (The Scripps Research Institute, La Jolla, CA, USA), including the removal of water molecules, addition of polar hydrogens, and assignment of Gasteiger charges. The processed structures were then converted to the PDBQT format. The small-molecule ligand VPA was energy-minimized using ADFRsuite-1.0, followed by the identification of rotatable bonds and assignment of Gasteiger partial charges before conversion to the PDBQT format. Molecular docking was carried out using the AutoDock Vina 1.2.0 software package (The Scripps Research Institute, La Jolla, CA, USA) (Detailed information is provided in the **Supplementary Table 1**) [21]. The AutoDock Vina docking score is the binding free energy (kcal/mol), with a lower score suggesting higher binding affinity. A docking energy of <–5 kcal/mol was considered indicative of relatively stable binding activity. Protein structural visualization was performed using PyMOL.

Softwares and Tools

Fig. 1 was assembled using Adobe Illustrator (version 29.5, 64-bit; Adobe Systems Incorporated, San Jose, CA, USA). Statistical plots in Figs. 2,4,5,6,7 were generated using R software (version 4.5.3; R Foundation for Statistical Computing, Vienna, Austria). Fig. 3 and the Venn diagrams were created using an online drawing tool (http://bioinformatics.psb.ugent.be/webtools/Venn/). Fig. 8 was generated using BioRender.com (https://www.biorender.com). All individual sub-panels were assembled, formatted, and composed into complete composite figures using Adobe Illustrator (version 29.5, 64-bit; Adobe Systems Incorporated, San Jose, CA, USA).

Results

Identification of DEGs

In the AD dataset (GSE5281), 4970 DEGs were identified, including 2410 up- and 2560 down-regulated genes. In the T2DM dataset (GSE76894), 392 DEGs were identified, 92 up- and 300 down-regulated. Visualization of DEGs from both datasets was carried out employing volcano plots and heatmaps (Fig. 1).

Identification of Key Genes in AD Samples Using WGCNA

The gene co-expression network was built using WGCNA, and the genes related to the AD phenotype were observed. To create a scale-free network, a soft threshold power of $\beta = 6$ ($R^2 = 0.85$) was selected (Fig. 2A). Modules were merged based on a cut-off value, resulting in 14 co-expression modules (Fig. 2B). The "lightyellow" module, consisting of 1865 genes, showed the strongest association with AD clinical traits (COR = –0.76, $p < 0.001$) and was considered the module most strongly associated with the AD phenotype (Fig. 2C,D). We identified 15 common genes by intersecting the AD module genes from WGCNA with the 4970 DEGs from the AD dataset (GSE5281) and the 392 DEGs from the T2DM dataset (GSE76894) (Fig. 2E).

Gene Functional Enrichment Analysis and Hub Gene Identification

To identify common regulatory pathways between AD and T2DM, GO biological process enrichment analysis and KEGG pathway analysis were performed. GO enrichment analysis identified 219 BPs, 43 MF, and 23 CC. At the BP level, the core differential genes were mainly enriched in gluconeogenesis, glycolysis, regulation of insulin secretion, ATP metabolic process, and regulation of neutrophil migration. At the MF level, the differential genes were mainly enriched in lyase activity, myosin heavy chain binding, filamin binding, glutamate receptor binding, and phosphotransferase activity with a phosphate group as acceptor. At the CC level, the DEGs were mainly enriched in

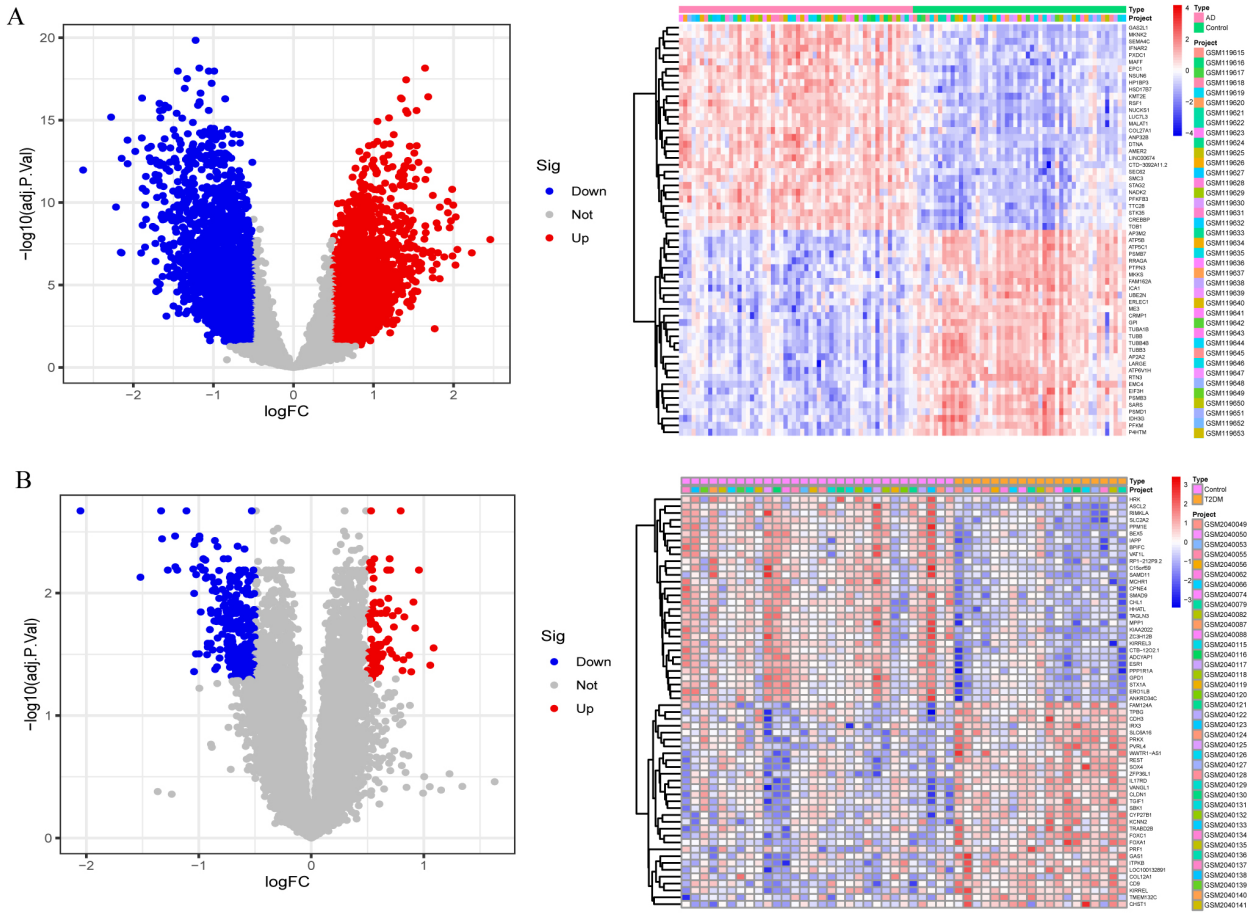

Fig. 1. Heatmap and volcano plot of DEGs in the GSE5281 and GSE76894 datasets. (A) Expression patterns of DEGs in patients with AD. (B) Expression patterns of DEGs in patients with T2DM. In the heatmaps, red and blue represent up-regulated and down-regulated mRNA expression, respectively. Darker colors indicate higher expression levels. DEGs, differentially expressed genes; AD, Alzheimer's disease; T2DM, type 2 diabetes mellitus.

presynaptic active zone membrane, distal axon, presynaptic active zone, synaptic membrane, and cell body membrane (Fig. 3A). KEGG enrichment analysis showed that the core differential genes were mainly enriched in glycolysis/gluconeogenesis, carbon metabolism, HIF-1 signaling pathway, MAPK signaling pathway, and pentose phosphate pathway (Fig. 3B).

The overall topological characteristics of the network showed that 42 genes were included, comprising the 15 core genes input into this study and 27 functionally related genes automatically supplemented by the platform based on functional associations. The top 10 hub genes with the highest connectivity were *DDC*, *CACNA2D2*, *STXBP1*, *SNAP25*, *ENO2*, *ALDOC*, *STX1A*, *CACNA1A*, *CACNA1E*, and *RBP4*. Among these, *STXBP1*, *SNAP25*, and *ENO2* had connectivity scores ≥10, indicating extensive interactions with core nodes and other genes. The functional association types among the genes included four categories: physical interaction (red lines, 89 connections), co-expression (purple lines, 102 connections), pathway association (light blue lines, 78 connections), and shared protein domains (light yellow lines, 47 connections) (Fig. 3C).

Machine Learning Screening of Core Module Genes

To identify the hub genes with the highest diagnostic value, LASSO, RF, SVM-RFE, and Boruta were used to cross-screen the 15 candidate genes for AD and T2DM. LASSO regression was applied using L1 regularization to compress redundant variables and select core feature genes. RF analysis was performed to further validate these selected genes. SVM-RFE and Boruta identified genes with significant classification ability via recursive elimination and shadow-feature testing, respectively (Fig. 4A–J). Venn diagrams were used for cross-comparison (Fig. 4K–M). Two genes, membrane palmitoylated protein 1 (*MPP1*) and enolase 2 (*ENO2*), were identified jointly by multiple algorithms.

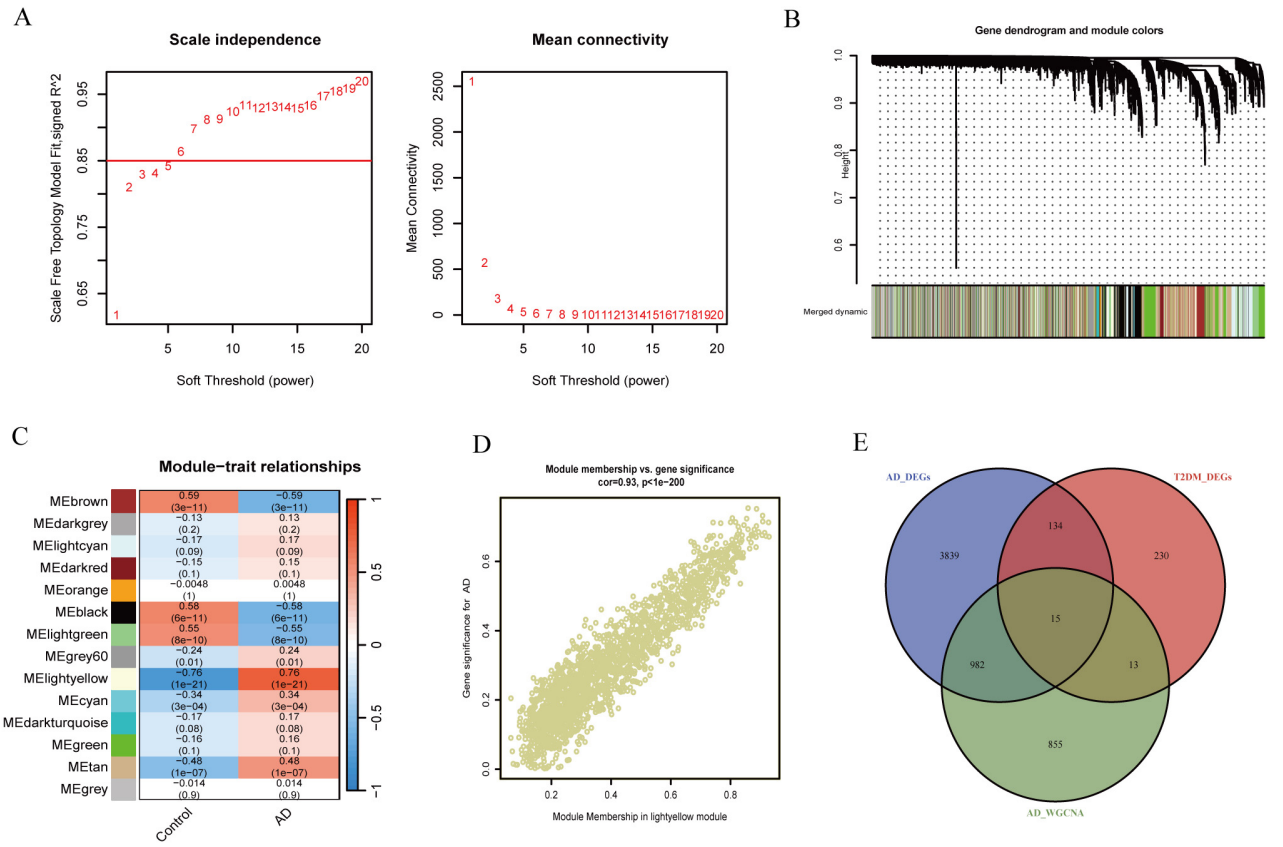

Fig. 2. Construction of the weighted gene co-expression network in AD. (A) Determination of the soft-thresholding power (β), including the scale-free topology fit index for different soft-threshold powers (left) and the average connectivity for different soft-threshold powers (right). (B) Dendrogram and fourteen co-expression modules of all DEGs clustered based on the dissimilarity measure (1-TOM), displayed in different colors. (C) Correlation analysis between gene modules and AD occurrence. (D) Scatter plot of module membership versus gene significance. (E) Venn diagram showing the 15 genes shared between AD and T2DM.

Validation of Core Module Gene Efficacy

Line plots and ROC curves were used further to validate the efficacy of the two key genes. The results showed that the hub genes exhibited significant diagnostic performance in both AD and T2DM. For AD, the AUC for *ENO2* was 0.883 (95% CI: 0.805−0.948), with an optimal cutoff value of 10.960, corresponding to a sensitivity of 0.929 and specificity of 0.804, while the AUC for *MPP1* was 0.905 (95% CI: 0.836−0.960), with an optimal cutoff value of 8.713, corresponding to a sensitivity of 0.946 and specificity of 0.804, respectively. For T2DM, the AUC for *ENO2* was 0.775 (95% CI: 0.633−0.895), with an optimal cutoff value of 11.472, corresponding to a sensitivity of 1.000 and specificity of 0.500, whereas the AUC for *MPP1* was 0.858 (95% CI: 0.742−0.946), with an optimal cutoff value of 9.204, corresponding to a sensitivity of 0.947 and specificity of 0.667, respectively. Calibration curves and decision curves showed that the model exhibited excellent calibration performance and stable clinical value across the entire range of risk thresholds (Fig. 5).

Gene Set Enrichment Analysis (GSEA)

We conducted GSEA to explore how the biomarkers affect the progression of AD and T2DM. The pathways significantly enriched in AD were associated with oxidative phosphorylation, citric acid cycle (TCA cycle), long-term potentiation/long-term depression, neuroactive ligand-receptor interaction, and leukocyte transendothelial migration (Fig. 6A–D). The pathways significantly enriched in T2DM were related to apoptosis, glycolysis/gluconeogenesis, leukocyte transendothelial migration, soluble N-ethylmaleimide-sensitive factor attachment protein receptor (SNARE) interactions in vesicular transport, and extracellular matrix-receptor interaction (Fig. 6E–H). Interestingly, several KEGG pathways were not only significantly enriched but also shared between AD and T2DM. These pathways were cytokine-cytokine receptor interaction, neuroactive ligand-receptor interaction, extracellular matrix-receptor interaction, leukocyte transendothelial migration, and the calcium signaling pathway.

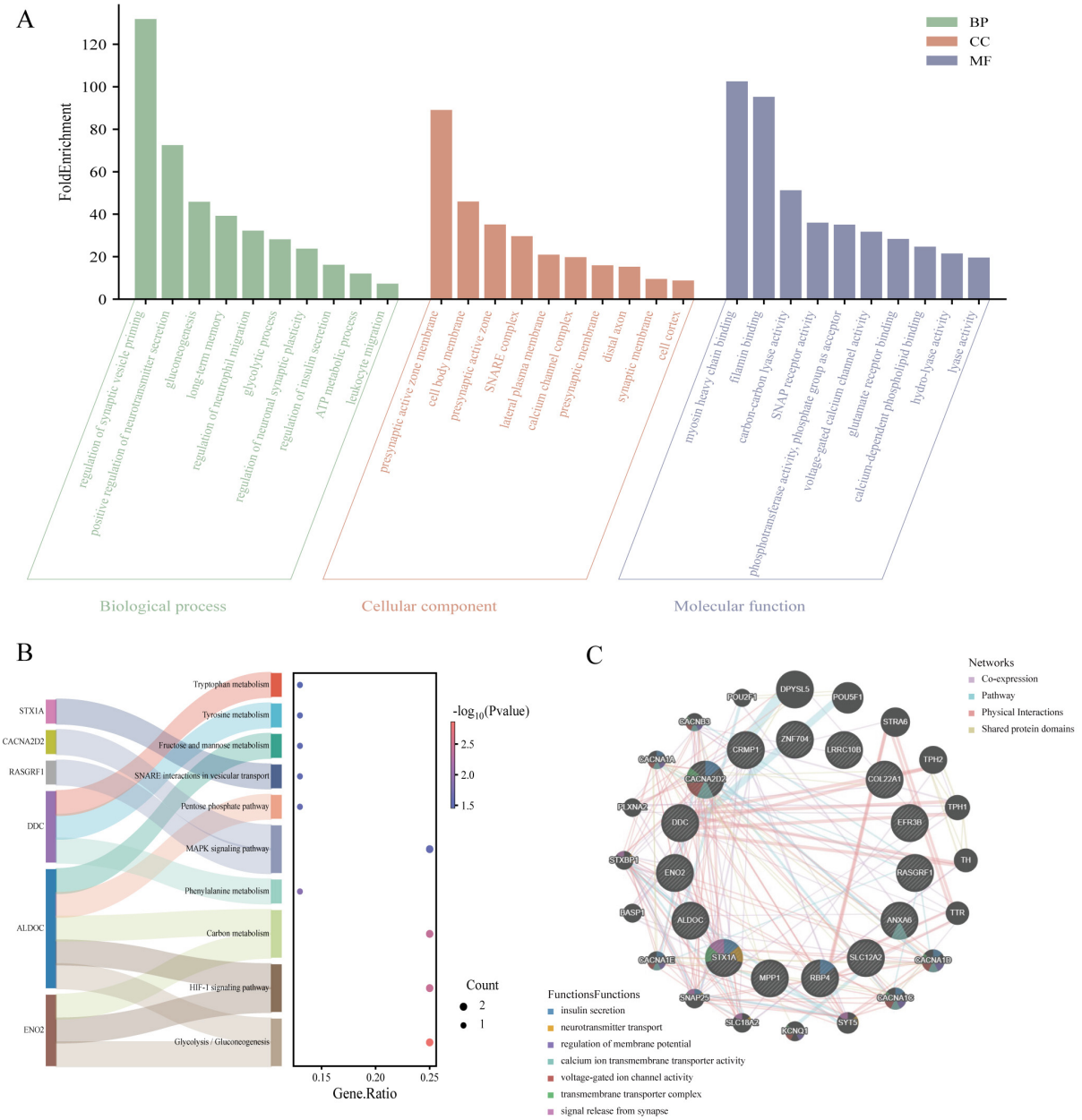

Fig. 3. GO and KEGG pathway enrichment analyses and gene functional interaction network. (A) GO functional enrichment and (B) KEGG pathway enrichment analysis of key genes. (C) Functional interaction network of key genes. Inner nodes represent the core genes included in this study, whereas outer nodes represent additional related genes obtained from public databases. Node size is proportional to the global interaction degree. BP, Biological Process; CC, Cellular Component; MF, Molecular Function; GO, Gene Ontology; KEGG, Kyoto Encyclopedia of Genes and Genomes.

ICI Analysis

The shared genes between AD and T2DM play a role in inflammatory responses and immune regulation. We further analyzed ICI in the AD and T2DM datasets. The results of immune infiltration analysis showed that *ENO2* expression was negatively correlated with monocytes and M2 macrophages in AD. The *MPP1* expression was positively correlated with gamma delta T (γδT) cells (Fig. 7A) and negatively correlated with M2 macrophages and activated dendritic cells. MPP1 expression was negatively correlated with neutrophils in T2DM (Fig. 7B). It should be noted that the LM22 signature was derived from peripheral blood leukocytes and may not fully capture tissue-resident immune cells in the brain or pancreatic islets. These results represent exploratory inferences about immune-related gene expression patterns.

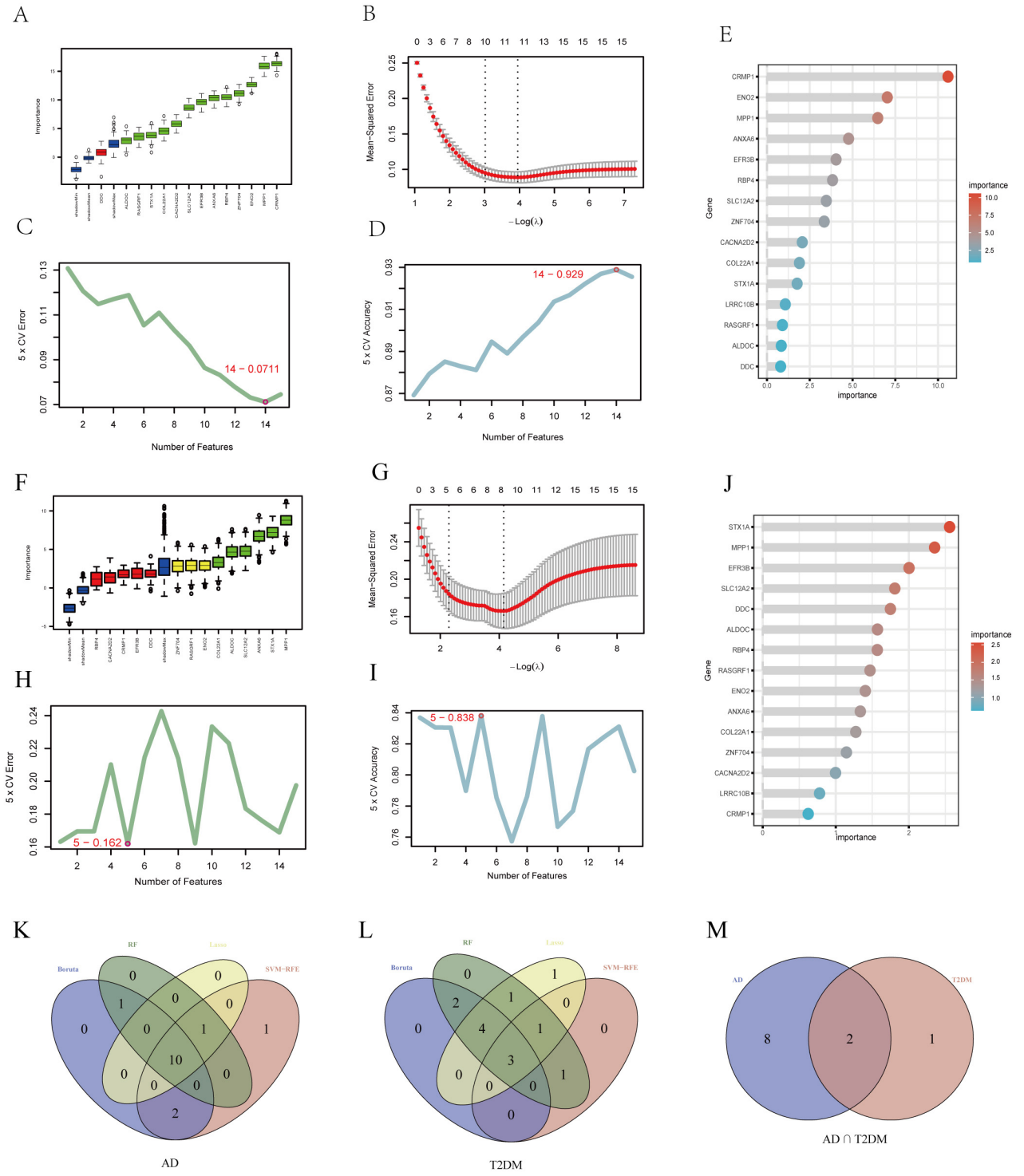

Fig. 4. Construction of four machine learning models for identifying key genes associated with AD and T2DM. Machine learning-based feature selection of 15 genes in (A–E) AD and (F–J) T2DM. (K–M) Venn diagram showing the overlapping key genes between AD and T2DM. RF, Random Forest; SVM-RFE, Support Vector Machine Recursive Feature Elimination.

Prediction of Candidate Drug

Potential compounds were screened using an interaction count with the core genes (*ENO2* and *MPP1*) of ≥3 as the threshold (Table 1). VPA is an antiepileptic drug that acts on the central nervous system. Environmental exposure-related compounds include bisphenol A, benzo(a)pyrene, sodium arsenite, and cadmium chloride. In addition, 4-(5-benzo(1,3)dioxol-5-yl-4-pyridin-2-yl-1H-imidazol-2-yl)benzamide was identified as an inhibitor of the TGF-β signaling pathway.

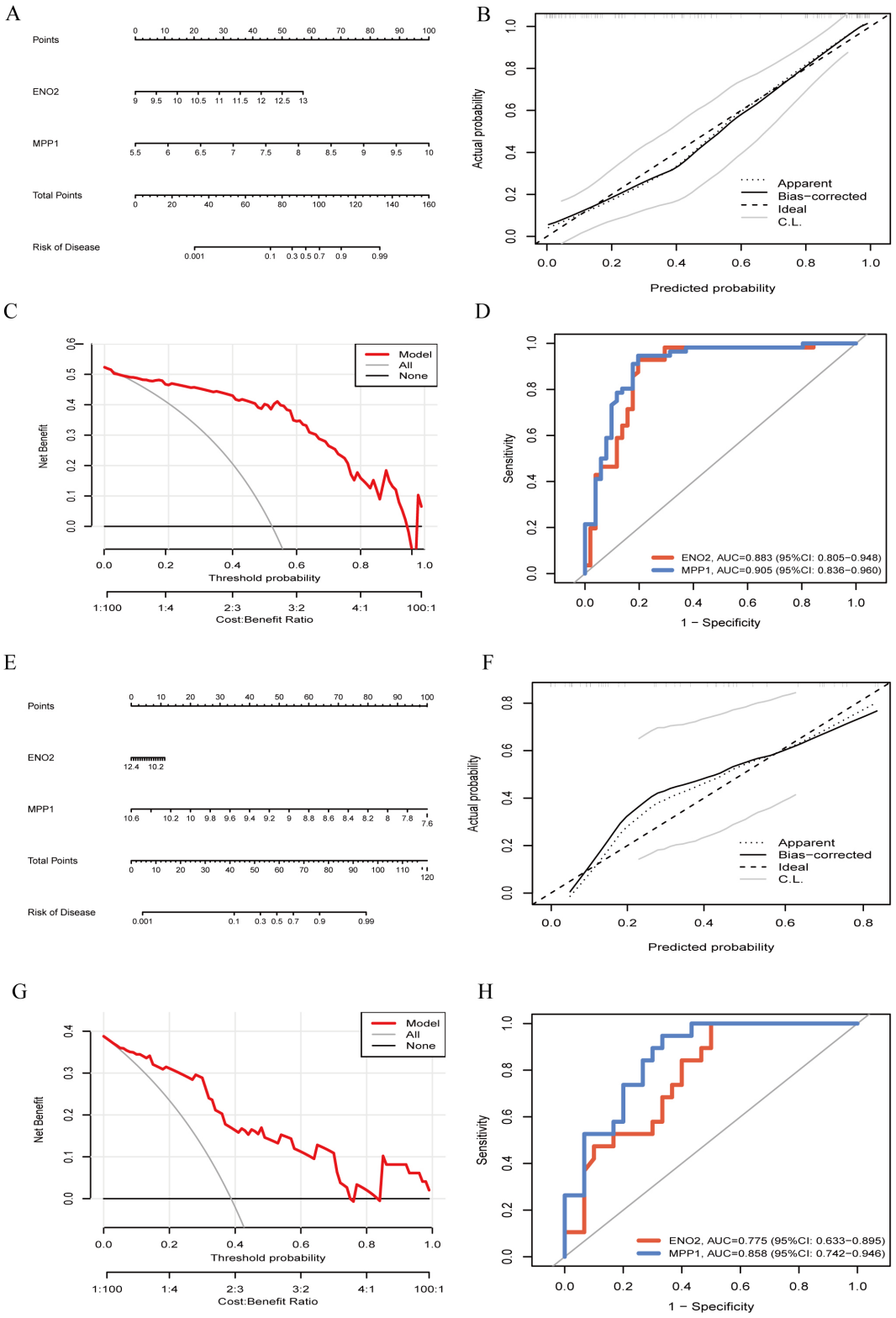

Fig. 5. Validation of four machine learning models in AD and T2DM. (A) Nomogram constructed using *ENO2* and *MPP1* for predicting AD risk. (B) Calibration curve of the nomogram. (C) Decision curve analysis (DCA) of the nomogram. (D) ROC curves of *ENO2* and *MPP1*. (E) Nomogram constructed using *ENO2* and *MPP1* for predicting T2DM risk. (F) Calibration curve of the nomogram. (G) DCA of the nomogram. (H) ROC curves of *ENO2* and *MPP1*.

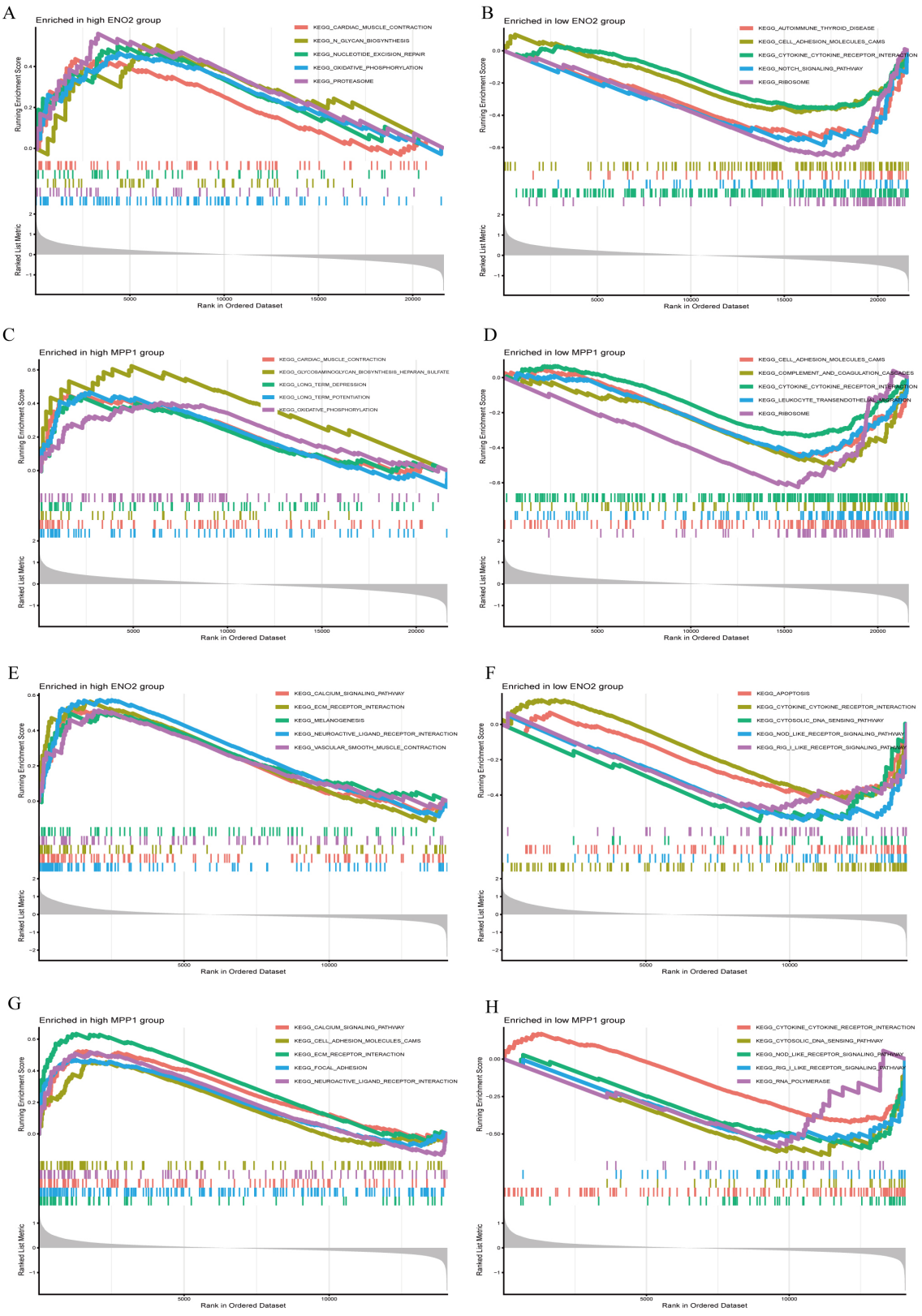

Fig. 6. Gene set enrichment analysis (GSEA). Pathways enriched in the (A) high-*ENO2*-expression, (B) low-*ENO2*-expression, (C) high-*MPP1*-expression, and (D) low-*MPP1*-expression subgroups in AD. Pathways enriched in the (E) high-*ENO2*-expression, (F) low-*ENO2*-expression, (G) high-*MPP1*-expression, and (H) low-*MPP1*-expression subgroups in T2DM.

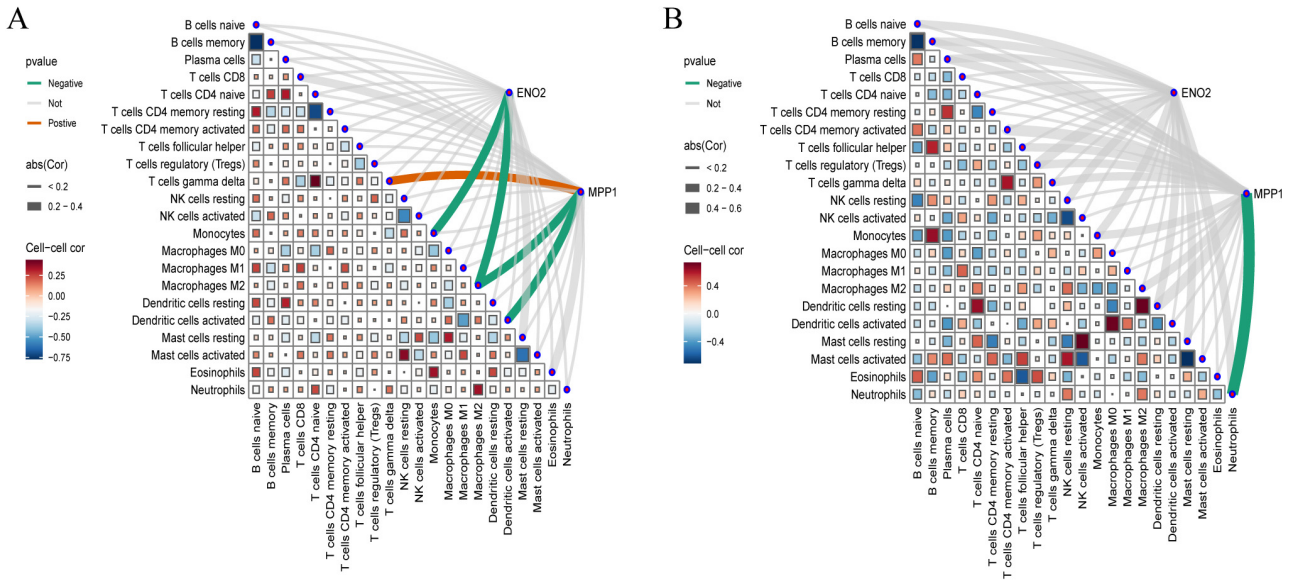

Fig. 7. Immune cell infiltration analysis. Correlation analysis between immune cells and *ENO2* and *MPP1* expression in (A) AD and (B) T2DM.

Table 1. Compounds predicted based on CTD.

Chemical name	Chemical ID	CAS RN	Interaction count in *ENO2*	Interaction count in *MPP1*
Bisphenol A	C006780	80-05-7	13	6
Benzo(a)pyrene	D001564	50-32-8	9	7
Valproic acid	D014635	99-66-1	8	4
Sodium arsenite	C017947	13768-07-5	5	3
4-(5-benzo(1,3)dioxol-5-yl-4-pyridin-2-yl-1H-imidazol-2-yl) benzamide	C459179	-	3	4
Cadmium chloride	D019256	10108-64-2	3	3

CTD, Comparative Toxicogenomics Database; *ENO2*, enolase 2; *MPP1*, membrane palmitoylated protein 1.

Molecular Docking

Molecular docking was conducted for the assessment of the affinity of drug candidates towards their targets and to determine their therapeutic potential in AD and T2DM. The targets *ENO2* and *MPP1* were docked with VPA. The binding free energies (ΔG, kcal/mol) of VPA with *ENO2* and *MPP1* were –4.747 kcal/mol and –5.346 kcal/mol, respectively (Fig. 8A). This indicated that VPA exhibited moderate binding affinity to *ENO2* and relatively stronger binding to *MPP1*, suggesting preferential targeting of *MPP1*. Structural characterization of the binding interfaces was further performed. In the VPA-*ENO2* complex, the ligand was located in the active pocket of *ENO2*. Two hydrogen bond interactions were found between the protein (residues GLN280 and ASN309) and the ligand (Fig. 8B). In the VPA-*MPP1* complex, VPA was also located in a defined binding pocket. The ligand was found to form hydrogen bond interactions with the ALA17 and MET14 residues of the protein (Fig. 8C).

Discussion

Bioinformatics and machine learning methods have been extensively applied over the past few years to identify important genes, biomarkers, and therapeutic targets in complex diseases, providing powerful tools to understand the molecular mechanisms of disease. AD is the most prevalent neurodegenerative disease, with its primary symptom of progressive cognitive decline, and poses a significant burden of disease upon public health. T2DM, being a chronic metabolic disease, has shown a continuously increasing prevalence and is strongly associated with cognitive decline and a higher risk of dementia. These two diseases frequently co-occur, and their potential association has attracted increasing attention.

While some previous studies based on bioinformatics techniques, including WGCNA, have investigated shared mechanisms between AD and T2DM, most of them have focused on screening shared pathways/hub genes from blood transcriptomic data [22]. Other studies have investigated

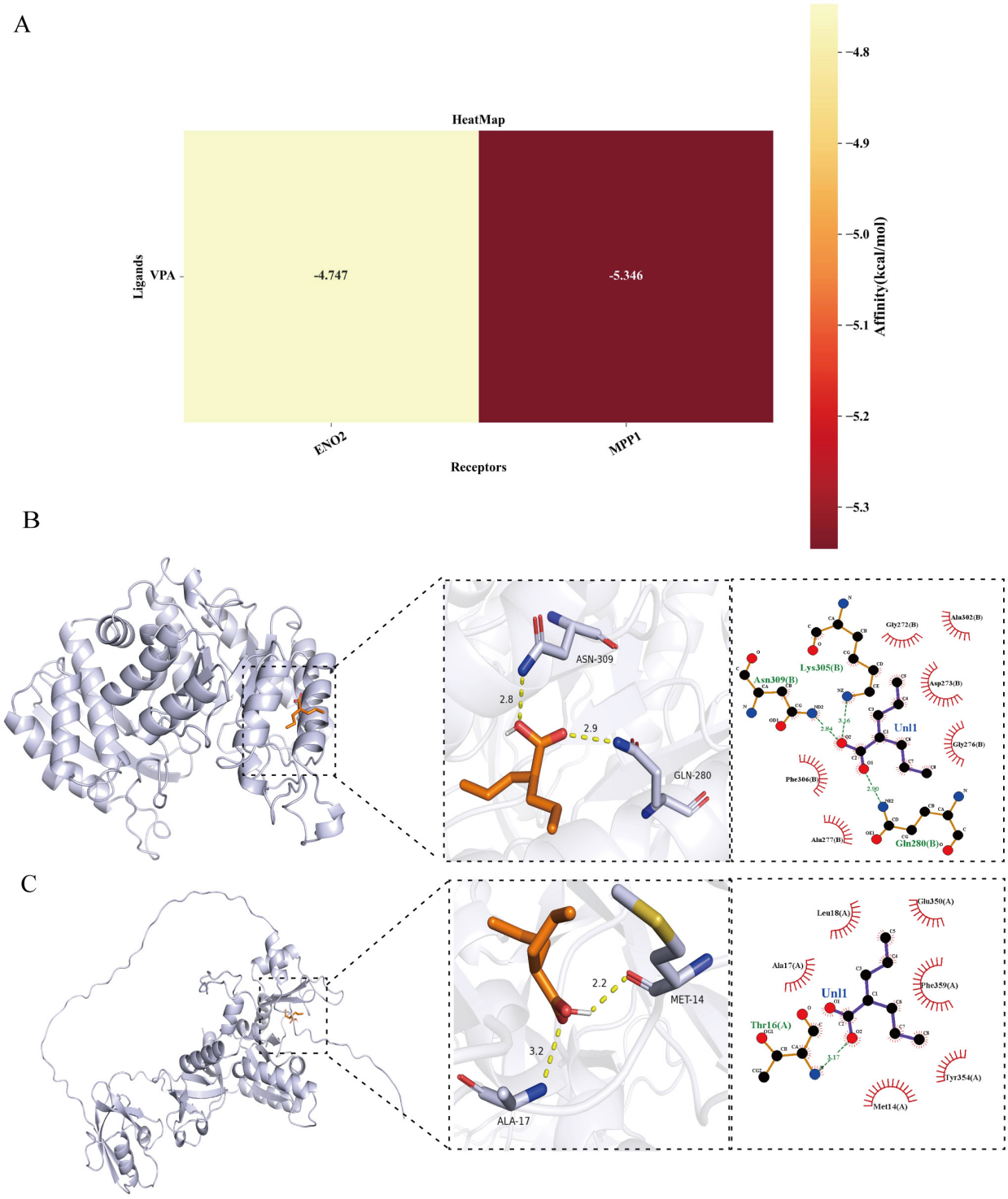

Fig. 8. Molecular docking analysis. (A) Heatmap matrix of docking binding energies. Molecular docking results of valproic acid with (B) *ENO2* and (C) *MPP1*.

shared mechanisms based on histological transcriptomic data, but focused on earlier stages and lacked machine learning cross-validation algorithms [23]. Thus, further investigation is still needed to elucidate the central molecular networks underlying the comorbidity of AD and T2DM.

In this study, we analyzed tissue-level transcriptomic information and then used four machine learning algorithms and immune infiltration analysis (CIBERSORT) to systematically identify the important molecular markers of AD-T2DM comorbidity. We identified *ENO2* and *MPP1* as

important biomarkers of AD-T2DM comorbidity. We also performed a systematic screening of compound-target interactions using the CTD. In this research, we aim to offer a novel theoretical foundation for understanding common molecular pathways in both diseases and for precision treatment.

A total of 4,970 DEGs were identified, of which 2410 were up-regulated and 2560 were down-regulated in the AD dataset (GSE5281). A total of 392 DEGs were obtained from the T2DM dataset (GSE76894), of which 92 genes were up-regulated while 300 genes were down-regulated. The "lightyellow" module was significantly negatively correlated with AD clinical traits, as revealed by the results of correlating the module with the traits using the WGCNA module-trait correlation analysis. The cross-over analysis of this module and the DEGs from AD and T2DM identified 15 genes shared between the two diseases.

Shared genes were primarily enriched in biological processes (including gluconeogenesis, glycolysis, regulation of insulin secretion, ATP metabolic process, and regulation of neutrophil migration) by GO enrichment analysis. For molecular functions, they were enriched in lyase activity, myosin heavy chain binding, filamin binding, glutamate receptors binding, and phosphotransferase activity with a phosphate group as an acceptor. For cellular components, they were enriched in the presynaptic active zone membrane, distal axon, presynaptic active zone, synaptic membrane, and cell body membrane. The core differential genes were significantly enriched in glycolysis/gluconeogenesis, carbon metabolism, HIF-1 signaling pathway, MAPK signaling pathway, and pentose phosphate pathway by the KEGG enrichment analysis. The glucose metabolism-related pathways enriched indicate that brain insulin resistance and impaired glucose utilization are potential drivers of the pathogenesis of AD. Low levels of glycolytic enzyme activity appear to be a key pathophysiological pathway involved in the comorbidity of AD and T2DM. Increased enrichment of synaptic membrane components and SNARE complexes suggests that there is an alteration in the structure and function of synapses in both T2DM and AD. Both membrane microdomain structure and vesicle secretion are impaired in the two diseases. A disruption of microdomains can occur simultaneously with disruptions in insulin signaling and neurotransmitter release. Furthermore, the enrichment of neutrophil migration regulation and leukocyte migration suggests that immune microenvironment dysregulation is involved in the progression of AD-T2DM comorbidity.

The four machine learning algorithms were then used for cross-screening, which revealed *ENO2* and *MPP1* as the core key genes for AD and T2DM, respectively. In the AD dataset, the AUC for *ENO2* and *MPP1* was 0.883 and 0.905, respectively. The AUCs were 0.775 and 0.858, respectively, suggesting very good cross-disease performance in the T2DM dataset. This cross-validation approach with multiple algorithms has been applied to many complex diseases to identify biomarkers and has great benefits for the reliability of the results.

The *ENO2* gene encodes neuron-specific enolase (NSE), also referred to as γ-enolase, and is located on human chromosome 12. *ENO2* is one of three isoenzymes of the enolase family and is predominantly found in mature neurons and neuroendocrine cells [24]. As a key enzyme of the glycolytic pathway, *ENO2* plays an important role in the energy metabolism of neurons by catalyzing the conversion of 2-phosphoglycerate to phosphoenolpyruvate. *ENO2* is not only glycolytic but also exhibits several non-enzymatic functions such as neuroprotection, neurotrophic factor-like activity, and regulation of neuroinflammation [24]. Furthermore, the C-terminal fragment of *ENO2* has been found to exert neuroprotective effects, promoting neuronal survival and axon growth [25]. A recent review by Liu et al. [26] shows that NSE is a useful tool to assess neuronal injury and is significantly correlated with early diagnosis, severity classification, and prognosis of cognitive dysfunction. A previous meta-analysis revealed that NSE levels in the cerebrospinal fluid were significantly higher in AD patients (Hedges' g = 0.822), which indicates that NSE is a good objective biochemical marker of neurodegeneration in AD [27]. *ENO2* was previously reported to be significantly downregulated in a single-cell sequencing study of oligodendrocytes from AD brains, suggesting that *ENO2* may be associated with AD pathology [28]. In T2DM patients, there is a strong correlation between serum NSE and diabetic peripheral neuropathy. In diabetic patients with diabetic peripheral neuropathy, the levels of serum *NSE* are significantly higher than in diabetic patients without neuropathy, with a positive correlation with the stage of neuropathy [29,30]. In one study, patients with diabetic retinopathy and mild cognitive impairment had significantly higher serum NSE levels, and NSE was a risk factor for mild cognitive impairment, suggesting that NSE could predict cognitive dysfunction associated with T2DM [31]. Therefore, *ENO2* can be used as a diagnostic marker and therapeutic target for the AD-T2DM comorbidity.

MPP1 (*p55*) is a member of the Membrane-Associated Guanylate Kinase protein family. It is primarily associated with the membrane cytoskeleton and has been shown to be palmitoylated and localize to lipid raft microdomains, where it plays a role in the lateral organization of the membrane, maintenance of mechanical stability, and signal transduction. *MPP1* contains PDZ (PSD-95, Discs large, Zonula occludens-1) and Src Homology 3 and guanylate kinase domains, enabling it to serve as a scaffold protein to coordinate the assembly of membrane protein complexes and mediate interactions with multiple cytoskeletal proteins [32,33]. The expression of *MPP1* is very high in the membranes and postsynaptic density fractions of the rat cerebral cortex. It binds to postsynaptic proteins, including Postsy-

naptic density protein 95, Calcium/calmodulin-dependent serine protein kinase, and Guanylate kinase-associated protein, and plays a role in early events in synaptogenesis [34]. *MPP1* is a hub gene in the pathological mechanism of depressive-like behavior and is involved in the p53 signaling pathway and long-term depression [35], suggesting that *MPP1* may regulate cognitive function through pathways related to synaptic plasticity. *MPP1* plays a vital role in the formation of lipid rafts at the cell membrane and in regulating the insulin signaling pathway. The normal start of the insulin receptor signaling depends strongly on the membrane lipid raft integrity. An abnormal lipid raft structure or composition is an important pathological correlation in the pathogenesis of insulin resistance [36]. *MPP1* function has been demonstrated to be required for activation of Harvey rat sarcoma virus Ras by insulin, and the inhibition of *MPP1* expression directly blocks the insulin signaling pathway from the insulin receptor [37]. In summary, *MPP1* dysfunction could simultaneously be responsible for reduced structural integrity of neurons and insulin resistance, thereby playing a vital role in the AD and T2DM comorbidity.

The CIBERSORT results should be interpreted with caution, as the LM22 signature reflects peripheral blood immune phenotypes and may not accurately capture tissue-resident immune cells. These findings are exploratory and require validation by immunohistochemistry or flow cytometry. We used GSEA to investigate the effects of *ENO2* and *MPP1* in AD and T2DM progression. The results revealed that these two genes affect distinct yet overlapping biological pathways in both diseases, such as leukocyte transendothelial migration, long-term potentiation/long-term depression, TCA cycle, oxidative phosphorylation, apoptosis, glycolysis/gluconeogenesis, SNARE interactions in vesicular transport, and axon guidance. These pathways are consistent with the GO and KEGG enrichment results, both of which support the results obtained.

ENO2 was found to be negatively correlated with monocytes and M2 macrophages in AD by immune infiltration analysis with CIBERSORT. Several studies reveal that *ENO2*, which is a marker of neuronal injury, is a valid indicator of the severity of injury, as evidenced by its changes in serum/cerebrospinal fluid concentration. Intracellular *ENO2* is neuroprotective, and extracellular release plays a potential role in the neuroinflammatory process [38]. The negative association with monocytes indicates that glycolytic metabolic reprogramming through the *ENO2* pathway could inhibit microglial phagocytosis, which might result in impaired clearance of Aβ and aggravation of neuroinflammation by changing the energy supply of the immune microenvironment.

The immunomodulatory function of *MPP1* in AD is more complex. *MPP1* was found to be positively correlated with γδT cells and negatively correlated with M2 macrophages and activated dendritic cells in this study. Neutrophils were negatively correlated with the expression of *MPP1* in T2DM. *MPP1* is known to be a key regulator of neutrophil polarity and migration [39]. Neutrophils can secrete elastase, which leads to insulin resistance and degradation of insulin receptor substrate-1, and are involved in the pathological mechanism of T2DM [40]. The negative correlation between *MPP1* and neutrophils may be associated with the effects of dexamethasone, a drug used in the treatment of T2DM, which downregulates the expression of *MPP1* in neutrophils, causing abnormal polarity and dysfunction. These alterations may contribute to chronic low-grade inflammation. Gamma delta T cells serve as a link between innate and adaptive immunity and have also attracted increasing attention as potential therapeutic targets in AD. In 3xTg-AD female mice, IL-17-positive γδ T cells were observed in the meninges and brain parenchyma during the early stages of AD, preceding the appearance of Aβ plaques and tau tangles, which indicates that the infiltration of γδ T cells is one of the early triggers of AD pathology [41]. The positive association between *MPP1* and γδ T cells suggests that *MPP1* could be involved in the regulation of neuroinflammatory activity of this immune cell subset by affecting membrane protein localization or signal transduction in γδ T cells. The specific associations of *ENO2* and *MPP1* with various subsets of immune cells obtained from CIBERSORT analysis in this study indicate that these two core genes may be involved in the complex immunoregulatory network of AD-T2DM comorbidity by metabolic reprogramming and functional polarization of immune cells.

Based on the CTD database, VPA was identified as a potential therapeutic agent for *ENO2* and *MPP1*. VPA belongs to the classic broad-spectrum antiepileptic drugs, which have been shown in recent years to possess several pharmacological activities, including neuroprotection, anti-inflammation, histone deacetylase (HDAC) inhibition, and glycogen synthase kinase-3 beta (GSK3β) inhibition [42]. In previous studies, VPA was found to decrease Aβ deposition and enhance cognitive function in the brain [43]. VPA is an HDAC inhibitor that may regulate GSK3β activity through epigenetic mechanisms, thus decreasing tau hyperphosphorylation and disrupting the vicious cycle of Aβ and tau pathologies [44]. VPA also acts as an HDAC3 inhibitor, which decreases neuroinflammation [45]. VPA's actions in T2DM include lowering insulin resistance, blood glucose, and HbA1C via HDAC inhibition, enhancing insulin signaling in the brain to normalize brain energy metabolism via FOXO1 inhibition [46], and preventing gluconeogenesis [47]. Furthermore, VPA activates autophagy, which can facilitate the removal of damaged proteins [48] and prevent damage caused by neurotoxins [49]. VPA could therefore be a good choice for the treatment of AD-T2DM, acting on both AD and T2DM.

The binding free energies of VPA with *ENO2* and *MPP1* were –4.747 kcal/mol and –5.346 kcal/mol, respectively, indicating a relatively high affinity for *MPP1*.

Based on structural analysis, it was proposed that VPA could bind within the ligand-binding groove of the PDZ domain of *MPP1* and compete with the binding of signaling molecules, thus affecting the organization of membrane lipid raft microdomains. In contrast, the interaction between VPA and *ENO2* may involve allosteric and indirect regulatory mechanisms. However, these docking predictions are based solely on computational simulations. The binding kinetic parameters should be further confirmed by experiments such as surface plasmon resonance and isothermal titration calorimetry, and the binding mechanism should be understood by site-directed mutagenesis and molecular dynamics simulations.

Although this study used a multi-algorithm integration and cross-validation approach to enhance the reliability of core gene screening, there are some limitations. First, the analyses were based on independent AD and T2DM cohorts rather than samples from patients with AD-T2DM comorbidity. Therefore, the identified shared genes represent molecular intersections inferred from separate disease contexts, and direct validation in AD-T2DM comorbid cohorts remains essential. Second, *ENO2* and *MPP1* have not yet been validated using single-cell sequencing data or other external independent datasets. Third, the drug intervention effects predicted based on the CTD database and the molecular docking results have not been validated *in vivo* or *in vitro*. Future studies should use single-cell sequencing and high-throughput microarray technologies to validate multidimensional data. Furthermore, animal and cellular models with the gene deletion or overexpression of *ENO2/MPP1* should be established by gene editing to elucidate the specific molecular mechanisms underlying VPA intervention in the context of AD-T2DM comorbidity, thereby facilitating the optimization of targeted therapeutic strategies.

Conclusion

In summary, the integrated application of WGCNA, machine learning algorithms, immune infiltration analysis, and molecular docking allowed the identification of *ENO2* and *MPP1* as shared molecular markers between AD and T2DM, while VPA was identified as a candidate compound warranting further investigation. *ENO2* and *MPP1* can act synergistically in the disease process of AD-T2DM comorbidity by regulating energy metabolism, synaptic function, and immune inflammation. This study offers a different theoretical basis and candidate targets for early detection, risk stratification, and precision intervention of AD-T2DM comorbidity. *ENO2* and *MPP1* should be clinically validated, and their functional mechanisms should be analyzed to facilitate targeted drug development and coordinated management of these two complex metabolic diseases in future research.

Availability of Data and Materials

The datasets analyzed in this study are publicly available. The Alzheimer's disease gene expression data can be found in the GEO under accession number GSE5281. The type 2 diabetes mellitus gene expression data can be found in the GEO under accession number GSE76894. The protein structure of *ENO2* was obtained from the PDB with ID 1TE6. The protein structure of *MPP1* was obtained from the AlphaFold Protein Structure Database (UniProt ID: Q00013). The drug target interaction data were retrieved from the CTD. Further information is available from the corresponding author upon reasonable request.

Author Contributions

TTL: Conceptualization, Methodology, Project administration, Writing – original draft, Writing – review & editing. HZW: Conceptualization, Methodology, Writing – review & editing. TL: Conceptualization, Methodology, Writing – original draft. LBZ: Conceptualization, Formal analysis, Supervision, Writing – review & editing. All authors have read and agreed to the published version of the manuscript. All authors have participated sufficiently in the work to take public responsibility for appropriate portions of the content and agreed to be accountable for all aspects of the work in ensuring that questions related to its accuracy or integrity.

Ethics Approval and Consent to Participate

Not applicable.

Acknowledgment

The authors acknowledge the GEO, PDB, AlphaFold DB, and CTD databases for providing open-access data and resources.

Funding

This work was financially supported by the Liaoning Provincial Natural Science Foundation Joint Fund Doctoral Research Start-up Project (2023-BSBA-219); the Open fund of Key Laboratory of Ministry of Education for TCM Viscera-State Theory and Applications, Liaoning University of Traditional Chinese Medicine (zyzx2307); the Project funded by China Postdoctoral Science Foundation (2023MD744221); and the Basic scientific research projects of colleges and universities in Liaoning Province (LJ222410162036).

Conflict of Interest

The authors declare no conflict of interest.

Supplementary Material

Supplementary material associated with this article can be found, in the online version, at https://doi.org/10.24976/Discov.Med.202638211.197.

References

[1] Better MA. Alzheimer's disease facts and figures. Alzheimer's & Dementia. 2023; 19: 1598–1695.

[2] Baviskar PS, Mahajan HS. Unveiling Alzheimer's disease (1901-2025): Historical insights, global burden, biological mechanisms, diagnostics, and therapeutic strategies. Ageing Research Reviews. 2026; 114: 102990. https://doi.org/10.1016/j.arr.2025.102990

[3] Genitsaridi I, Salpea P, Salim A, Sajjadi SF, Tomic D, James S, et al. 11th edition of the IDF Diabetes Atlas: global, regional, and national diabetes prevalence estimates for 2024 and projections for 2050. The Lancet. Diabetes & Endocrinology. 2026; 14: 149–156. https://doi.org/10.1016/S2213-8587(25)00299-2

[4] Janson J, Laedtke T, Parisi JE, O'Brien P, Petersen RC, Butler PC. Increased risk of type 2 diabetes in Alzheimer disease. Diabetes. 2004; 53: 474–481. https://doi.org/10.2337/diabetes.53.2.474

[5] Lanctôt KL, Hviid Hahn-Pedersen J, Eichinger CS, Freeman C, Clark A, Tarazona LRS, et al. Burden of Illness in People with Alzheimer's Disease: A Systematic Review of Epidemiology, Comorbidities and Mortality. The Journal of Prevention of Alzheimer's Disease. 2024; 11: 97–107. https://doi.org/10.14283/jpad.2023.61

[6] Simó R, Ciudin A, Simó-Servat O, Hernández C. Cognitive impairment and dementia: a new emerging complication of type 2 diabetes-The diabetologist's perspective. Acta Diabetologica. 2017; 54: 417–424. https://doi.org/10.1007/s00592-017-0970-5

[7] Cao F, Yang F, Li J, Guo W, Zhang C, Gao F, et al. The relationship between diabetes and the dementia risk: a meta-analysis. Diabetology & Metabolic Syndrome. 2024; 16: 101. https://doi.org/10.1186/s13098-024-01346-4

[8] Waqas SA, Ali D, Khan TM, Qureshi S, Siddiqui H, Sajid M, et al. Trends in Alzheimer's-Related Mortality Among Type 2 Diabetes Patients in the United States: 1999-2019. Endocrinology, Diabetes & Metabolism. 2025; 8: e70032. https://doi.org/10.1002/edm2.70032

[9] Madhusudhanan J, Suresh G, Devanathan V. Neurodegeneration in type 2 diabetes: Alzheimer's as a case study. Brain and Behavior. 2020; 10: e01577. https://doi.org/10.1002/brb3.1577

[10] Diniz Pereira J, Gomes Fraga V, Morais Santos AL, Carvalho MDG, Caramelli P, Braga Gomes K. Alzheimer's disease and type 2 diabetes mellitus: A systematic review of proteomic studies. Journal of Neurochemistry. 2021; 156: 753–776. https://doi.org/10.1111/jnc.15166

[11] Karki R, Kodamullil AT, Hofmann-Apitius M. Comorbidity Analysis between Alzheimer's Disease and Type 2 Diabetes Mellitus (T2DM) Based on Shared Pathways and the Role of T2DM Drugs. Journal of Alzheimer's Disease : JAD. 2017; 60: 721–731. https://doi.org/10.3233/JAD-170440

[12] Kakkar A, Singh H, Jasoria Y, Kumar A, Chopra S, Chopra H, et al. Bridging pathologies: Mechanistic insights into the diabetes-Alzheimer's nexus. EXCLI Journal. 2026; 25: 261–289. https://doi.org/10.17179/excli2025-9165

[13] Tonda-Turo C, Origlia N, Mattu C, Accorroni A, Chiono V. Current Limitations in the Treatment of Parkinson's and Alzheimer's Diseases: State-of-the-Art and Future Perspective of Polymeric Carriers. Current Medicinal Chemistry. 2018; 25: 5755–5771. https://doi.org/10.2174/0929867325666180221125759

[14] Samaras K, Makkar S, Crawford JD, Kochan NA, Wen W, Draper B, et al. Metformin Use Is Associated With Slowed Cognitive Decline and Reduced Incident Dementia in Older Adults With Type 2 Diabetes: The Sydney Memory and Ageing Study. Diabetes Care. 2020; 43: 2691–2701. https://doi.org/10.2337/dc20-0892

[15] Kim HK, Biessels GJ, Yu MH, Hong N, Lee YH, Lee BW, et al. SGLT2 Inhibitor Use and Risk of Dementia and Parkinson Disease Among Patients With Type 2 Diabetes. Neurology. 2024; 103: e209805. https://doi.org/10.1212/WNL.0000000000209805

[16] Nowell J, Blunt E, Gupta D, Edison P. Antidiabetic agents as a novel treatment for Alzheimer's and Parkinson's disease. Ageing Research Reviews. 2023; 89: 101979. https://doi.org/10.1016/j.arr.2023.101979

[17] Goodarzi G, Tehrani SS, Fana SE, Moradi-Sardareh H, Panahi G, Maniati M, et al. Crosstalk between Alzheimer's disease and diabetes: a focus on anti-diabetic drugs. Metabolic Brain Disease. 2023; 38: 1769–1800. https://doi.org/10.1007/s11011-023-01225-3

[18] Zhang C, Luo Z, Ji L. Identification of potential diagnostic markers and molecular mechanisms of asthma and ulcerative colitis based on bioinformatics and machine learning. Frontiers in Molecular Biosciences. 2025; 12: 1554304. https://doi.org/10.3389/fmolb.2025.1554304

[19] Li H, Yu B, Yuan Y, Chen N, Guo H, Zhang H, et al. Integrated computational analysis of molecular mechanisms underlying perfluorooctane sulfonic acid induced thyroid toxicity. Scientific Reports. 2025; 15: 7920. https://doi.org/10.1038/s41598-025-92678-2

[20] Chai G, Brewer JM, Lovelace LL, Aoki T, Minor W, Lebioda L. Expression, purification and the 1.8 angstroms resolution crystal structure of human neuron specific enolase. Journal of Molecular Biology. 2004; 341: 1015–1021. https://doi.org/10.1016/j.jmb.2004.05.068

[21] Eberhardt J, Santos-Martins D, Tillack AF, Forli S. AutoDock Vina 1.2.0: New Docking Methods, Expanded Force Field, and Python Bindings. Journal of Chemical Information and Modeling. 2021; 61: 3891–3898. https://doi.org/10.1021/acs.jcim.1c00203

[22] Ye XW, Liu MN, Wang X, Cheng SQ, Li CS, Bai YY, et al. Exploring the common pathogenesis of Alzheimer's disease and type 2 diabetes mellitus *via* microarray data analysis. Frontiers in Aging Neuroscience. 2023; 15: 1071391. https://doi.org/10.3389/fnagi.2023.1071391

[23] Zhu Y, Ding X, She Z, Bai X, Nie Z, Wang F, et al. Exploring Shared Pathogenesis of Alzheimer's Disease and Type 2 Diabetes Mellitus via Co-expression Networks Analysis. Current Alzheimer Research. 2020; 17: 566–575. https://doi.org/10.2174/1567205017666200810164932

[24] Horvat S, Kos J, Pišlar A. Multifunctional roles of γ-enolase in the central nervous system: more than a neuronal marker. Cell & Bioscience. 2024; 14: 61. https://doi.org/10.1186/s13578-024-01240-6

[25] Hafner A, Obermajer N, Kos J. γ-Enolase C-terminal peptide promotes cell survival and neurite outgrowth by activation of the PI3K/Akt and MAPK/ERK signalling pathways. The Biochemical Journal. 2012; 443: 439–450. https://doi.org/10.1042/BJ20111351

[26] Liu F, Li H, Hong X, Liu Y, Yu Z. Research progress of neuron-specific enolase in cognitive disorder: a mini review. Frontiers in Human Neuroscience. 2024; 18: 1392519. https://doi.org/10.3389/fnhum.2024.1392519

[27] Katayama T, Sawada J, Takahashi K, Yahara O, Hasebe N. Meta-analysis of cerebrospinal fluid neuron-specific enolase levels in Alzheimer's disease, Parkinson's disease, dementia

with Lewy bodies, and multiple system atrophy. Alzheimer's Research & Therapy. 2021; 13: 163. https://doi.org/10.1186/s13195-021-00907-3

[28] Saito ER, Miller JB, Harari O, Cruchaga C, Mihindukulasuriya KA, Kauwe JSK, et al. Alzheimer's disease alters oligodendrocytic glycolytic and ketolytic gene expression. Alzheimer's & Dementia : the Journal of the Alzheimer's Association. 2021; 17: 1474–1486. https://doi.org/10.1002/alz.12310

[29] Li J, Zhang H, Xie M, Yan L, Chen J, Wang H. NSE, a potential biomarker, is closely connected to diabetic peripheral neuropathy. Diabetes Care. 2013; 36: 3405–3410. https://doi.org/10.2337/dc13-0590

[30] Pusapati LCV, V P, V SS, Nallaperumal S, Vannan I. Association Between Serum Neuron-specific Enolase Levels and Diabetic Neuropathy in Patients With Diabetes Mellitus: A Cross-sectional Study. Cureus. 2025; 17: e87214. https://doi.org/10.7759/cureus.87214

[31] Yu ZW, Liu R, Li X, Wang Y, Fu YH, Li HY, et al. High Serum Neuron-Specific Enolase Level Is Associated with Mild Cognitive Impairment in Patients with Diabetic Retinopathy. Diabetes, Metabolic Syndrome and Obesity : Targets and Therapy. 2020; 13: 1359–1365. https://doi.org/10.2147/DMSO.S249126

[32] Biernatowska A, Olszewska P, Grzymajło K, Drabik D, Kraszewski S, Sikorski AF, et al. Molecular characterization of direct interactions between MPP1 and flotillins. Scientific Reports. 2021; 11: 14751. https://doi.org/10.1038/s41598-021-93982-3

[33] Biernatowska A, Wójtowicz K, Trombik T, Sikorski AF, Czogalla A. MPP1 Determines the Mobility of Flotillins and Controls the Confinement of Raft-Associated Molecules. Cells. 2022; 11: 311. https://doi.org/10.3390/cells11030311

[34] Jing-Ping Z, Tian QB, Sakagami H, Kondo H, Endo S, Suzuki T. p55 protein is a member of PSD scaffold proteins in the rat brain and interacts with various PSD proteins. Brain Research. Molecular Brain Research. 2005; 135: 204–216. https://doi.org/10.1016/j.molbrainres.2004.12.023

[35] Liu W, Huang Z, Xia J, Cui Z, Li L, Qi Z, et al. Gene expression profile associated with Asmt knockout-induced depression-like behaviors and exercise effects in mouse hypothalamus. Bioscience Reports. 2022; 42: BSR20220800. https://doi.org/10.1042/BSR20220800

[36] Inokuchi JI. Insulin resistance as a membrane microdomain disorder. Biological & Pharmaceutical Bulletin. 2006; 29: 1532–1537. https://doi.org/10.1248/bpb.29.1532

[37] Podkalicka J, Biernatowska A, Olszewska P, Tabaczar S, Sikorski AF. The microdomain-organizing protein MPP1 is required for insulin-stimulated activation of H-Ras. Oncotarget. 2018; 9: 18410–18421. https://doi.org/10.18632/oncotarget.24847

[38] Haque A, Polcyn R, Matzelle D, Banik NL. New Insights into the Role of Neuron-Specific Enolase in Neuro-Inflammation, Neurodegeneration, and Neuroprotection. Brain Sciences. 2018; 8: 33. https://doi.org/10.3390/brainsci8020033

[39] Quinn BJ, Welch EJ, Kim AC, Lokuta MA, Huttenlocher A, Khan AA, et al. Erythrocyte scaffolding protein p55/MPP1 functions as an essential regulator of neutrophil polarity. Proceedings of the National Academy of Sciences of the United States of America. 2009; 106: 19842–19847. https://doi.org/10.1073/pnas.0906761106

[40] Talukdar S, Oh DY, Bandyopadhyay G, Li D, Xu J, McNelis J, et al. Neutrophils mediate insulin resistance in mice fed a high-fat diet through secreted elastase. Nature Medicine. 2012; 18: 1407–1412. https://doi.org/10.1038/nm.2885

[41] Brigas HC, Ribeiro M, Coelho JE, Gomes R, Gomez-Murcia V, Carvalho K, et al. IL-17 triggers the onset of cognitive and synaptic deficits in early stages of Alzheimer's disease. Cell Reports. 2021; 36: 109574. https://doi.org/10.1016/j.celrep.2021.109574

[42] Markowicz-Piasecka M, Miłkowska Z, Adla SK, Huttunen KM, Pietrzak B. Beyond epilepsy: The expanding role of valproic acid in Alzheimer disease therapy - a review. The Journal of Pharmacology and Experimental Therapeutics. 2025; 392: 103658. https://doi.org/10.1016/j.jpet.2025.103658

[43] Xuan AG, Pan XB, Wei P, Ji WD, Zhang WJ, Liu JH, et al. Valproic acid alleviates memory deficits and attenuates amyloid-β deposition in transgenic mouse model of Alzheimer's disease. Molecular Neurobiology. 2015; 51: 300–312. https://doi.org/10.1007/s12035-014-8751-4

[44] Rekha A, Afzal M, Babu MA, Menon SV, Nathiya D, Supriya S, et al. GSK-3β dysregulation in aging: Implications for tau pathology and Alzheimer's disease progression. Molecular and Cellular Neurosciences. 2025; 133: 104005. https://doi.org/10.1016/j.mcn.2025.104005

[45] Tribble JR, Kastanaki E, Uslular AB, Rutigliani C, Enz TJ, Williams PA. Valproic Acid Reduces Neuroinflammation to Provide Retinal Ganglion Cell Neuroprotection in the Retina Axotomy Model. Frontiers in Cell and Developmental Biology. 2022; 10: 903436. https://doi.org/10.3389/fcell.2022.903436

[46] Khan S, Kumar S, Jena G. Valproic acid reduces insulin-resistance, fat deposition and FOXO1-mediated gluconeogenesis in type-2 diabetic rat. Biochimie. 2016; 125: 42–52. https://doi.org/10.1016/j.biochi.2016.02.014

[47] Kellar D, Craft S. Brain insulin resistance in Alzheimer's disease and related disorders: mechanisms and therapeutic approaches. The Lancet. Neurology. 2020; 19: 758–766. https://doi.org/10.1016/S1474-4422(20)30231-3

[48] Gaffke L, Firyn N, Rintz E, Pierzynowska K, Piotrowska E, Mazur-Marzec H, et al. Therapeutic potential of lithium chloride and valproic acid against neuronopathic types of mucopolysaccharidoses through induction of the autophagy process. Archives of Biochemistry and Biophysics. 2023; 747: 109754. https://doi.org/10.1016/j.abb.2023.109754

[49] Zhang Y, Wu JY, Weng LH, Li XX, Yu LJ, Xu Y. Valproic acid protects against MPP^+-mediated neurotoxicity in SH-SY5Y Cells through autophagy. Neuroscience Letters. 2017; 638: 60–68. https://doi.org/10.1016/j.neulet.2016.12.017